Simulation of a Light Aircraft Encountering a Helicopter Wake

Y. Wang* M. White† and G.N. Barakos‡

School of Engineering, University of Liverpool, Liverpool, L63 3GH, UK

P. Tormey§ and P. Pantazopoulou¶

Civil Aviation Authority, UK

Three different methods of modelling helicopter wakes namely a prescribed wake, a free wake and a CFD actuator disk, are presented and compared with available wind tunnel and flight test data. The free wake model was then used to generate the wake vortices of a helicopter hover-taxing over an airport runway. The Beddoes prescribed wake model, with a wake decay law, was also used to generate the far wake of a helicopter in level flight. The wake induced velocity fields were integrated into an aircraft flight dynamics model and piloted flight simulations were carried out to study a light aircraft encountering a helicopter wake during landing and level flight. It was found that for the current landing wake encounter scenario, the existing wake encounter criteria and severity metrics for the determination of the hazardous distance might not be appropriate if the wake encounter occurs close to the ground. The landing simulation results suggest that for a helicopter in low-speed hover-taxiing (less than 40 kt airspeed), the wake encounter detectable horizontal distance is about three times the diameter of the rotor, which coincides with the current safety guidelines of the Civil Aviation Authority of the UK. The level flight simulations revealed the effects of the vertical separation distance and of the wake decay on the encounter severity.

Nomenclature

A	Rotor disk area, πR^2 (ft^2)
C_t	Rotor thrust coefficient, $T/0.5\rho V_t^2 A$
D	Rotor diameter (ft)
h	Helicopter rotor hub height (ft)
R	Rotor radius (ft)
T	Helicopter rotor thrust (N)
V	Helicopter forward speed (ft/s)

*Research Fellow, Department of Engineering. Email: yxwang@liverpool.ac.uk

†Lecturer, Department of Engineering. Email: mdw@liverpool.ac.uk

‡Professor, Member of AIAA, Department of Engineering. Email: G.Barakos@Liverpool.ac.uk

§Civil Aviation Authority. Email: Peter.Tormey@caa.co.uk

¶Civil Aviation Authority. Email: P.Pantazopoulou@caa.co.uk

V_t Rotor tip speed, ΩR (ft/s)

β Wake angle to the centreline of the runway (deg)

μ Advance ratio, V/V_t

Ω Rotor rotational speed (rad/s)

I. Introduction

The wakes of fixed-wing aircraft and helicopters are often studied in aviation, and one of the areas of interest is the examination of the separation distance or separation time criteria used for the prevention of aircraft wake encounters. There are clear definitions of the separation time or distance for the wake encounter between fixed-wing aircraft.[1,2] However, for the wake encounter between a helicopter and an encountering light aircraft, the separation distance is not clearly defined. There is some guidance for helicopter wake encounters, for example, the three-rotor-diameter separation distance described in the CAP 493, Manual of Air traffic Services.[1] However, serious and fatal accidents have happened when a light aircraft has encountered a helicopter wake and the pilot has lost control.[3,4] The wake generated by a helicopter is different to that of a fixed-wing aircraft; helicopter wake vortices can be more intense than those of a fixed-wing aircraft of a similar weight with different flow structures, duration and decay.[1,2] Helicopter wake vortices depend on the type of the helicopter (weight, size, and configuration) and its operating conditions (altitude, velocity). Helicopter wake encounter accidents have happened around airports where a helicopter is in a hover or hover taxi regime and the light aircraft is performing a landing or departure. In either case, both the helicopter and the fixed-wing aircraft are at low altitudes and relatively low speeds. When a helicopter is flying at low altitude, ground effect can distort its wake vortices and a low forward speed causes a large wake skew angle. All of these features are different to that of the available helicopter fly-by LIDAR measurement wake data[5,6] where helicopters are at higher altitudes and at higher forward speeds. For a landing aircraft, because of its proximity to the ground, even a small wake upset could cause a severe hazard. In this circumstance, the current wake encounter criteria might not be suitable.

Flight probe tests and fly-by measurement data for a landing aircraft encountering a helicopter wake are scarce and difficult to conduct. Doppler LIght Detection And Ranging (LIDAR) was used by Kopp[6] to measure the wake vortices generated by military aircraft and rotorcraft. The measurements were mainly focused on the roll-up phase of the vortices. One of the fly-by LIDAR measurements obtained was for the wake of a Puma helicopter. The tangential velocity profiles of the port vortices at two time instances and the decay of the maximum tangential velocity were reported. These data provided a reference for the validation of various wake models. Another flight test investigation of rotorcraft wake vortices in forward flight was carried out by Teager et al.[5] Different rotorcraft were used, and the wake vortex strength and decay characteristics were calculated from the LIDAR measurements. The detectability and hazard distances for small aircraft behind helicopters were established based on the flight test data. However, all the Laser Doppler Velocimeter (LDV) measurements were for helicopter airspeeds above 40 knots.

Flight simulation can play an important role in the prediction and assessment of wake encounter hazards. It is a safe, low cost and controllable method of investigation. However, wake encounter simulation has its own requirements in order to be a useful tool, and a wake model is essential for the generation of wake velocity data. In addition, a validated aircraft flight dynamic model is necessary and the wake velocity data has to be carefully integrated into the simulation system to account for the interference of the wake on the aircraft flight dynamics when a wake encounter occurs. Piloted simulation trials are needed to assess the

severity of wake encounter, and a high level of fidelity of the visual cues is also very important to reflect the real wake encounter scene.

The objectives of the work presented in this paper were: (1) to study and compare different numerical models to generate helicopter rotor wake, from prescribed wake models to free wake models and more complex CFD-based modelling. (2) to use the selected wake models to calculate the wake induced velocity field from a rotorcraft, and to integrate it into an aircraft flight dynamics model to carry out piloted wake encounter simulation trials in a flight simulator. The aim of the flight simulation testing is to answer the following questions:

- What level of disturbances can a helicopter wake cause on an approaching light aircraft?
- What effect do the altitude off the ground and speed have on the hazard of an encounter?
- How does the manner in which the wake is encountered i.e., encounter angle and offset between the helicopter and the aircraft, change the aircraft hazard upset and hence the level of safety?

In this paper, three helicopter wake models are presented together with comparisons against wind tunnel or field measurements. The wake encounter simulation set-up, test conditions and parameters are then described, followed by the results of the simulation trials and the conclusions related to separation distances.

II. Helicopter wake modelling

Prediction and simulation of helicopter rotor wakes, including wake vortex geometry, wake age and wake induced velocity flow-fields, are vital to wake encounter simulation research. There are various helicopter wake models available in the literature[7] with different levels of complexity and fidelity. Three wake modelling methods are used in this study. These are a prescribed wake model, a free wake model and a CFD actuator disk model.

II.A. Prescribed wake models

Prescribed wake models[7,8] have been developed to enable predictions of the inflow characteristics through the rotor disk. These models prescribe the locations of the rotor tip vortices as functions of wake age on the basis of experimental observations. For hovering flight, the Landgrebe, Kocurek and Tangler models are widely used,[7] whilst the Beddoes generalised wake model is used for forward flight.[7,8] The basic premise of the Beddoes model is that the lateral and longitudinal distortions from a helical sweep are small in comparison to the vertical distortions. These distortions can then be related to the velocity distribution over the rotor disk. The prescription of the vertical displacement of the tip vortices is given by empirical weighting functions. The Beddoes wake model was used for this study to calculate the rolled up tip vortex core positions, the induced velocity field being estimated using the Biot-Savart law. The wake vortices were modelled on a 4-bladed rotor at 0.1 forward advance ratio (μ), which is the ratio of the forward speed to the rotor tip speed, and the results are shown in Fig. 1(a).

II.B. Free wake models

In the free wake model,[7,9] the initial geometry of wake is assumed. The wake itself is represented by a large number of free vortex filaments. These filaments can propagate freely in the induced velocity field. A free wake model has been developed in this study to account for ground effect and to produce a more

realistic vortex strength, and hence the induced downwash velocity vectors for the simulation. The influence of ground effect is one of the most important factors that have to be considered when simulating helicopter flight near the ground during a hover taxi. In this wake model, the rotor blade is represented by a line vortex from root to tip and root vortex effects are ignored. The total rotor lift is assumed to be equal to the weight of helicopter and the circulation of the wake vortex equals the circulation of the blade it is trailed off. The self-induced flow and the local wake curvature, as well as the effect of a fuselage, are considered in the formulation. The velocity field is estimated using the Biot-Savart law. Ground effect is simulated by using a mirror wake with respect to the ground.[9] Figure 1(b) shows iso-surfaces of vorticity, which indicates the positions of the vortex cores, as predicted by the free wake model.

II.C. CFD actuator disk models

In a CFD actuator disk (AD) model, the Navier-Stokes equations are solved along with turbulence models to simulate the flow field. The rotor itself is simulated by using an actuator disk, which is added into the CFD domain as a momentum source to simulate a pressure jump over the rotor. In this study the AD method is implemented by using the HMB flow solver.[10] The solver uses a cell-centred finite volume approach combined with an implicit dual-time method. Osher's upwind scheme is used to resolve the convective fluxes. A central differencing spatial discretisation method is used to solve the viscous terms. A Generalised Conjugate Gradient (GCG) method is used in conjunction with a Block Incomplete Lower-Upper (BILU) factorisation as a pre-conditioner to solve the linearised system of equations, which is obtained from a linearisation in pseudo-time. The flow solver can be used in serial or parallel mode.[10] For the CFD actuator disk model, the mesh and blocks were generated using the ICEMCFD[11] tool. A drum was created to enclose the actuator disk, and sliding planes[10] were used to account for relative motion. The wake generated by the CFD actuator disk is shown in Figs. 1(c) and 1(d), where stream-traces are used to illustrate the wake geometry.

III. Validation of the wake models

Heyson,[12] amongst others, have measured the induced velocity fields near a lifting rotor. The teetering type rotor consisted of two untwisted blades with a NACA 0012 aerofoil section. The rotor radius was 7.5 ft and the tip speed was 500 fts^{-1}. His measurements included the velocity fields at several positions downstream of the rotor. The wind tunnel test set-up, and the measured velocity planes are shown in Fig. 2. The Beddoes prescribed model, the free wake model and the actuator disk model have been applied using Heyson's test conditions and rotor parameters. In a wake encounter study, the main focus is on the wake in the downstream region (mid-wake and far-wake) of the rotor. Comparisons of these methods with Heyson's wind tunnel data are shown in Fig. 3, where the velocities at two transverse planes (yz plane) at x/R=2 and x/R=3 (downstream) are compared, where R is the rotor radius. These were the positions furthest downstream of the rotor where data were available. At x/R=2, all three models showed reasonable agreement in the vertical planes until z/R=0.5. Further away from the rotor, where the induced velocity was lower, the Beddoes and free wake models over-predicted the velocity. The AD model still predicted well in the inboard wake region but a large difference was found in the outboard area, particularly around the two shoulders. Further downstream at x/R=3, where wake is more developed, the agreement was improved. The velocity field was well predicted by the three models in the vertical planes up to z/R=0.7. Generally speaking, the CFD actuator disk model showed the best predictions among the three wake models but with

the highest computational cost.

Fly-by Doppler LIDAR measurements of a Puma helicopter wake were given by Kopp.[6] The tangential velocities on the port-side of the rotor were measured at approximately 9 seconds after their generation. The helicopter forward airspeed was 65 kts so the measurement position was about $20D$, where D is the rotor diameter, downstream from the rotor center. Far wake or long age wake CFD simulation is a significant challenge because it requires high density grids and needs to overcome numerical dissipation.[13] A CFD actuator disk model and the Beddoes model were applied to the flight condition of Kopp's test. The measured maximum velocity decay over a long wake age was also presented and is reproduced in Fig. 4. The wake vortex decay is indicated by the decrease of the maximum tangential velocity measured near the port vortex core over the passing-by time. During the first 10 seconds, the vortex maintains its strength, which is followed by a near linear decay after 10 seconds. From this decay, the velocity magnitudes can be deduced at different ages or downstream distances. Comparisons of the tangential velocity distributions using the AD model are shown in Fig. 5, where the results of different CFD grid densities are plotted together to reveal the grid sensitivity. The finest grid (22 million cells) produced reasonably good agreement with the fly-by test data in the far downstream region up to $6D$ from the rotor center. Further downstream, the CFD grid needs to be increased significantly, which is not a viable approach to generate wake data for the proposed real time flight simulation.

The Beddoes model was developed mainly from the near-wake wind tunnel measurements and in itself has no wake decay. To extend it to the far-wake, the above mentioned wake decay relation was applied to the Beddoes wake model to produce wake simulations at long wake ages. The results are shown in Fig. 5, where the tangential velocity distributions at different downstream positions are presented. At the far downstream position of $20D$ from the rotor, the velocity field was well predicted.

It was impractical to apply the free wake model to simulate the far field wake of the above mentioned Puma helicopter tests. Because the current study was focused on the wake of a hovering or hover-taxiing helicopter close to ground, it was considered appropriate to compare the free wake model against any flight tests conducted near ground. Matayoshi et al.[14] presented some wake velocity measurements of a helicopter hovering close to ground. In their flight tests, the MuPAL-ϵ helicopter hovered over the anemometers at a height of 60–80ft (Fig. 6) and the wake velocities were measured using a MELCO LIDAR[14] and ultrasonic anemometers. The free wake was applied to the MuPAL-ϵ helicopter using the same parameters as those in the flight test. The comparison of wake velocities generated by the free wake model and measured by LIDAR and anemometers are shown in Fig. 6. Notice that the LIDAR measurements was spatially averaged over a range bin length of 30 m[14] and the existence of a difference of peak and trough velocities indicates there might be a nature wind during the measurements, which biased the velocity field. After taking these factors into consideration, the free wake model results were considered to be in reasonable agreement with those from the LIDAR and anemometer measurements.

IV. Induced velocity flow field

The free wake model was selected to generate the wake data for the wake encounter simulation after balancing the accuracy and computational cost of the three wake models. A Dauphin helicopter configuration was used in the wake encounter simulation because it is considered as a light helicopter.[1,2] The wake induced velocity vectors were calculated from the Biot-Savart law after the wake vortex elements were determined from the free wake model. The rotor hub was set at the origin (0, 0, 0) of the coordinate system along a

runway centreline over the runway threshold. The induced velocity field covers a box of $x = -20$ ft to 320 ft (about 8 rotor diameters), $y = -50$ ft to 50 ft and $z = -50$ ft to 30 ft. The induced velocity field at different advance ratios is shown in Fig. 7, where the wake geometry and three planes of velocity vectors and downwash contours at 0 (the rotor hub centre), $1D$ and $3D$ downstream are displayed.

The oblique wake encounter is shown in Fig. 8, where the orientation angle is set to 45 and the helicopter rotor hub is also offset 2 rotor diameters from the runway centreline. The wake induced velocity field of the Dauphin helicopter at a lower height (h) of 20 ft is also shown in Fig. 8. In this case, the influence of the ground effect was more pronounced.

The Beddoes wake model, with the measured wake decay, was also applied to the Dauphin helicopter rotor to generate the far-wake flow fields. The induced flow flow fields and the wake geometry are shown in Fig. 9 for the baseline wake (no decay) and for the wake with a 50% decay.

V. Wake encounter flight simulation

The piloted wake encounter flight simulations were carried out in the HELIFLIGHT simulator[15] at the University of Liverpool by two test pilots and two student pilots. The wake encountering aircraft is a general aviation (GA) training aircraft configured to be similar to a Grob Tutor aircraft. During the simulation the rolling/pitching/yawing moments, aircraft altitude change, velocities and accelerations during an encounter were recorded, together with the pilot's control inputs, to capture a complete description of the encounter. These data provided a quantitative measure of the effect of the wake on the aircraft. After each set of runs the pilot was asked to rate the hazard using the Wake Vortex Severity Rating Scale.[16]

V.A. Wake encounter Scenarios

The first scenario was designed for helicopter wake encounters during the approach and landing phase, as shown in Fig. 10, where the Dauphin helicopter was offset to the centreline of the runway near the runway threshold when the GA aircraft was approaching to land. The response of the aircraft to the wake and the perceived hazard of the pilot to the encounter were measured for different advance ratios, orientation angles, and encounter heights at the maximum rotor thrust coefficient (C_t) of 0.013.

The wake of the helicopter was placed at the position over the runway that caused the aircraft to fly through it whilst on a standard approach profile (see Fig. 11). For a helicopter hover-taxiing around a runway, the forward speed is normally low, hence three different air speeds of 0 (hover), 20 kts, and 40 kts were chosen. The corresponding advance ratios were 0.0 (hover), 0.05 and 0.1. The helicopter was positioned at two heights of 50 ft and 20 ft, and the orientation of the wake was adjusted by varying the angle of the wake to the runway and its lateral offset from the runway axis. The different wake angles (β) caused the aircraft to encounter the wake at oblique angles whilst the offset caused interactions of the aircraft lifting surfaces with the wake at different stages of wake evolution.

The second scenario was designed for helicopter wake encounter during level flight. In this case, the Dauphin helicopter was positioned at a height of 200 ft and had a forward speed of 65 kt (advance ratio of 0.15). The GA aircraft was flown behind the helicopter to penetrate the helicopter wake in parallel at different altitudes to investigate the effects of the vertical distance between the helicopter and the encountering aircraft. The wake induced velocities at 100% (baseline), 90%, 75% and 50% of wake strengths were used in the simulations to study the effect of the wake age or decay. In each run the pilot was asked to fly into the wake at a specific height.

In these flight simulations, the helicopter wake is artificially "frozen" in space without the consideration of the helicopter motion. The results therefore represent the worst case scenarios where the encounters occur when the helicopter wake vortex is at its full strength. The encounter effects in a real scenario may differ considerably and may be less significant because of the relative movement between the encountering aircraft and the helicopter. Consideration of the worst case scenario is also required in studies related to the development of flight safety regulations where conservative approaches should be adopted.

V.B. Simulator, aircraft flight dynamics model and pilot rating scale

The simulator used in the trials is the HELIFLIGHT simulator (shown in Fig. 10). It is a full motion simulator with a single-seat cockpit. There are three-collimated visual display channels for the Out-the-Window view and two chin-window displays. The generic cockpit has representative flight instruments. Control sticks, pedal and engine throttle are provided by a dynamic control loading system to resemble the controls of a fixed-wing GA aircraft. It has a six DOF full motion platform and the pilot is able to communicate with the control room at all times via a headset.

The aircraft flight dynamics model was developed in the FLIGHTLAB[17,18] simulation package based on a Grob Tutor configuration. The main aircraft components of the wing, fuselage, propeller, tail, fin, landing gears, engine and control system were modelled. Wake interference on the aircraft was integrated into the dynamics model as velocity look-up tables, which produced additional angles of attack and sideslip on the wings, fuselage, propellers, tail, fin and other lifting surfaces.

During the trials, the pilot was asked to give feedback on the wake encounters and rate the severity according to a wake vortex encounter pilot rating scale, which is a scale that has been used in previous wake encounter studies by Padfield et al.[16] The rating scale is shown in Fig. 12. It is a simple decision tree that enables the pilots to provide a subjective assessment of the effect of the wake encounter and their ability to recover.

V.C. Test procedure

For each test condition, the pilots were asked to fly the GA aircraft along a 3°glide slope path aiming to land the aircraft at a specified touchdown point for the landing scenario, or to fly at a specific altitude for the level flight scenario. The wake was placed at specific positions according to the test matrix. The pilot was not informed whether the wake was present or not. In each simulation sortie, the pilot was asked to give wake encounter severity ratings if the wake was detected. In addition to the rating, other parameters related to the aircraft dynamics, positions and pilot control activities were also recorded for further analysis. Typically, several runs of the same test condition were carried out to obtain consistent results.

VI. Simulation results and discussion

VI.A. Helicopter wake encounter during a landing

VI.A.1. Vortex upset hazard

The helicopter wake vortex induced disturbances were probed by the GA light aircraft in the simulation to obtain a direct assessment of wake vortex hazard as a function of distance behind the wake generating helicopter. In addition to the pilot's awarded wake encounter severity rating and comments, the aircraft dynamic response parameters can be used to assess the wake vortex upset hazard.

The criteria for test pilot assessments are dependent on the manner in which the assessment evolved.[5] For fixed-wing aircraft encounters, generalised criteria need to be used during an approach to determine the limits of upsets (roll, pitch, yaw and any acceleration) that would permit the continuation of the approaching rather than a go-around. The amount of control used and the most severe aircraft excursions that the pilots would tolerate need to be considered.[5] For a more definitive criterion, a rule of thumb has evolved that suggested that the maximum acceptable bank angle at published minimums would be that obtained by dividing 1200 by the wingspan in feet.[5] For a Boeing 747 it equates to 6°of bank, while for smaller aircraft like Grob Tutor (10 meter wing span), it is approximately 35°. Normally the hazardous roll angle limit was rounded off to 30°. The hazard distance was defined by Teager[5] as the distance at which a nominal 30°bank upset is caused.

In a helicopter wake encounter, the perceived severity of the hazard caused by the wake vortex on the encountering aircraft depends on the height and the speed of the helicopter and the vortex age, which is reflected in terms of the distance of the encounter behind the wake generating helicopter.

The time-history plots of the aircraft responses and pilot control activity in a typical wake encounter case are shown in Fig. 13. The left-hand figures show the dynamic responses of aircraft attitude of roll, pitch and yaw angles, rates and accelerations. The pilot's control activities of the lateral, longitudinal sticks and the pedal, the altitude of the aircraft and the body accelerations in x, y and z body axes are plotted in the right-hand column of figures. The aircraft encounters the wake at approximately 47 seconds. The pilot gave this wake encounter an "F" rating, which represents a hazardous encounter, for landing scenario. The pilot commented that if the wake encounter had happened at a higher altitude, then the rating would have been a "D".

In the current landing simulations, the aircraft bank angle did not exceed 30°even for the most severely rated upset encounter. However, the test pilot gave an "F" rating for some of the encounters, which means, in his opinion, the safety of flight was compromised and the hazard is intolerable. The reason that the pilot gave such a high rating is because during the phase of landing the aircraft is close to the ground, where there is little room to manoeuvre the aircraft even if the vortex upset is relatively small. The 30°bank angle criterion might not be as well suited to wake encounters during landing.

Another criterion for the wake encounter is the vortex upset detectability distance at which the impact of the helicopter's wake vortex can be detected by the approaching aircraft. The data of the above test case are re-plotted in Fig. 14, where the horizontal distance (X) between the aircraft and the helicopter was used. The position of three times the rotor diameter was also indicated on the plots. The helicopter was positioned at the runway threshold (X=0) and at a height of 50 ft. The GA aircraft approached landing on a 3°flight path. The roll acceleration and vertical (Z) body acceleration started to show abrupt changes at a distance of about 120 ft ($3D$) from the helicopter position. At a distance of about 80 ft ($2D$) the accelerations in pitch appeared. The peak of roll attitude rate was $21°s^{-1}$ and peak roll angle was about 14°. A similar pitch rate appeared later and the maximum pitch angle was 16°. A smaller yaw acceleration, yaw rate and yaw angle were also observed in the plots. The pilot applied lateral control to compensate the roll disturbance, and later longitudinal and pedal controls were also applied.

VI.A.2. Helicopter advance ratio

A higher advance ratio causes a smaller wake skew angle and the wake vortex extends further downstream. Fig. 15 shows the roll dynamic response, vertical acceleration and lateral control inputs at helicopter air-

speeds of 0 (hover), 20 kt and 40 kt. The roll acceleration and rate plots indicated that the wake encounter detectability distances were at about 120 ft ($3D$), 70 ft ($1.8D$) and 30 ft ($0.8D$) for the three conditions. Larger roll accelerations and rates were produced in the lower air speed cases as the encounter occurred closer to the helicopter. However, the largest roll angle, lateral control displacement and vertical body accelerations were generated at the highest air speed of 40 kt. The pilots awarded ratings of "C" and "B" to the hover and the 20 kt airspeed cases.

VI.A.3. Effect of helicopter offset

When the helicopter was re-located away from the centre line of the runway, the distance between the induced velocity calculation points and the wake vortex elements was increased. Dependent on the offset distance, in some regions the induced velocity would be reduced. It also might cause a partial encounter, which means that only a portion of the aircraft is affected by the wake. These effects are shown in Fig. 16, where the roll dynamic response, lateral control inputs and vertical acceleration at three offsets are compared. The least upsets in the dynamic responses and lateral control inputs were generated at the $2D$ offset encounter and a rating of "A" was awarded, which indicated that the wake vortex was shifted away from the runway area and its effect was barely discernible. The upsets caused in the $1D$ offset case is still large because of the partial encounter and resulted in a "C" rating. The changes of the signs in the roll angle, the roll rate and acceleration and the lateral control indicated that the encounter was different to that of the no offset case.

VI.A.4. Wake encountering angles

The wake encounter angle changes the orientation between the wake vortex to the fixed induced velocity field. It is anticipated that the resulting wake induced velocity distribution would be altered when compared with the parallel (zero angle) encounter case. The effect of the encounter angle is shown in Fig. 17, where the roll dynamic responses, lateral control and vertical acceleration are compared. The wakes were positioned at a offset of $1D$ from the runway centreline. The oblique encounters (45°) caused the least upsets in the roll angle and the lateral control and a "B" rating was awarded. This is partly because the fact that the wake vortex was skewed away from the center line of the induced velocity field, which increased the distance between the vortex elements and the induced velocity calculation points. This larger distance reduced the induced velocity and hence generated less of an upset. In the crossing encounter (90°), the shortest detectability distance about 30 ft ($0.75D$) was found. The detectability distances were 120 ft ($3D$) and 90 ft ($2.3D$) for the parallel and the oblique encounters and a "C" rating was awarded for both.

VI.A.5. Helicopter altitude

For the landing wake encounter, simulation trials were also conducted at a lower altitude of 20 ft ($0.5D$). In this case the ground effect is expected to be more pronounced, which would produce a different induced velocity field to the out ground effect cases. A comparison with the higher altitude case is shown in Fig. 18. The lower altitude caused similar levels of roll rate and acceleration on the encounter aircraft as that of the higher altitude. However, the maximum roll angle was significant smaller than that of the higher altitude case. A lower severity rating of "B" was awarded to the lower altitude case.

VI.B. Helicopter wake encounter during level flight

VI.B.1. Vortex upset hazard

The simulation results of the helicopter wake encounter during level flight are shown in Fig. 19, where the time-history plots of the aircraft responses and pilot control inputs are presented. The aircraft flew into the wake at the same level (altitude) as the helicopter. The results indicated that the maximum disturbed roll angle of the aircraft reached to 45°. The pilot applied up to 97% of the available lateral control to compensate for the roll upset. The wake also caused a nearly 18°yaw displacement and up to 33% pedal was applied by the pilot. The roll rate and acceleration started at about 45.7 seconds, corresponding to a distance of about 300 ft ($7.5D$) from the rotor center. The pilot gave this wake encounter severity a "G" rating, meaning that the excursion of the aircraft states was sufficiently high that safe recovery could not be assured.

VI.B.2. Helicopter height and aircraft altitude

In the level fight simulation, the pilots were asked to fly the GA aircraft to penetrate the helicopter wake at different altitudes to investigate the effects of the vertical distance between the helicopter and the encountering aircraft. The wake is skewed when the helicopter is flying at a forward speed of 65 kt (μ=0.15). The wake induced velocity field is highly dependent on not only the horizontal distance but also the vertical distance. The results are shown in Fig. 20. In the baseline case (altitude of 200 ft), the GA aircraft was flying at the same height as the Dauphin helicopter and the wake caused the largest disturbances in the roll axis. The lower the altitude of the aircraft was, the less roll upsets were produced. The control inputs were also reduced at the lower altitude. At an altitude of 120 ft, the vertical distance between the helicopter and the GA aircraft was about $2D$, the wake caused a maximum roll angle of 9°and the pilot had to apply up to 46% of the lateral control to recover the attitude. In this case the pilot awarded a "C" severity rating.

VI.B.3. Helicopter wake decay

Wake decay reduces the wake vortex strength (circulation) and hence decreases the induced velocities. Level flight wake encountering simulations were also carried out at the 100% (no wake decay), 90%, 75% and 50% of the baseline wake strength to study the wake decay effect. The results are shown in Fig. 21. The maximum roll angles caused by the wake at these four wake strengths are 45°, 26°, 15°and 2°, respectively. Compared with the baseline case, the wake at the 50% baseline wake strength caused little upset, and almost no additional control was needed for recovery; a "B" rating was awarded. While at the 75% wake strength, up to 66% of the lateral control was required and resulted in an "E" rating. The required lateral control went to 70% at the 90% wake strength, in which case the pilot awarded an "F" rating.

VII. Conclusions

Three different methods of modelling a helicopter wake namely a prescribed wake model, a free wake model and a CFD actuator disk model, have been developed and validated with wind tunnel experimental measurements and flight test data. The free wake model was used to generate the wake vortices of a light helicopter in hover-taxing over an airport runway. The wake induced velocity fields were integrated into an aircraft flight dynamics model based on a Grob Tutor configuration. Piloted flight simulations were carried out to study the severity of helicopter wake encounters.

The wake encounter parameters of helicopter altitude, forward speed, orientation angle and offset to the runway centerline were investigated in the simulations. In each simulation sortie, subjective pilot wake encounter severity rating and objective aircraft dynamic responses and pilot control activities were used to quantify the effects of the helicopter's wake.

For the low altitude and relatively low forward speed hover-taxing helicopter wake encounter, the rotor wake is confined in the vicinity of helicopter. So in these simulations, the generated wake encounter upset was generally "mild" and the bank angle never exceeded the 30°hazard criterion. However, in some test cases, the pilot rated the wake encounter as an "F", which means, in his opinion, the safety of flight was compromised. The reason is because during the phase of landing the aircraft is close to the ground, where there is little room to manoeuvre the aircraft even the vortex upset is small. Hence the 30°bank angle criterion, which was developed for the high attitude and speed flight, might not be suited for the wake encounters during landing.

The simulations revealed that helicopter advance ratio, altitude, wake encountering orientation angle and offset to the centreline of runway all had influences on the encountering aircraft. This preliminary study suggests that for the current landing wake encounter scenario, where the helicopter is in low-speed hover-taxiing, the detectable horizontal distance is about three times the diameter of the rotor, which coincides with the current safety guidelines of the Civil Aviation Authority.

For the helicopter wake encounter during level flight, the vertical distance between the helicopter and the aircraft is an important parameter to determine the encounter severity. It was found that at a vertical distance of $2D$, the wake still caused a rating "C" severity on the encountering aircraft. The simulations indicated that under the current test conditions, the wake upsets reduced to insignificant levels after the wake was decayed to 50% of its full strength.

It is recognised that neither the number of the pilots nor the number of trials are sufficient in this wake encounter simulation study. Future simulation trials that include more test pilots are needed to enhance the existing datasets and perhaps, lead to a more informed set of criteria for the separation of light fixed-wing aircraft and helicopter.

Acknowledgements

The financial support from the Civil Aviation Authority (CAA) UK and the University of Liverpool is gratefully acknowledged.

References

[1]CAA, "CAP 493: Manual of Air Traffic Services Part 1," Tech. Rep. 4, Civil Aviation Authority, November 2011.

[2]Wilson, P. and Lang, S., "Technical Report to Support the Safety Case for Recategorization of ICAO Wake Turbulence Standards: Proposed Wake Turbulence Categories for All Aircraft Commonly Provided with Air Traffic Service," Tech. Rep. 0, EUROCONTROL and FAA, April 2011.

[3]CAA, "Aircraft Accident Report 1/93," Tech. rep., Civil Aviation Authority, 1993.

[4]Wilson, P., Lepadatu, C., Barnes, S., and Lang, S., "Technical Report to Support the Safety Case for Recategorization of ICAO Wake Turbulence Standards: An Overview of Key Aviation Accidents Sometimes Assumed to Have Been Caused by Wake Turbulence," Tech. Rep. 0.1, EUROCONTROL and FAA, December 2010.

[5]Teager, S., Biehl, K., Garodz, L., Tymczyszym, J., and Burnham, D., "Flight Test Investigation of Rotorcraft Wake Vortices in Forward Flight," Tech. Rep. DOT/FAA/CT-94/117, FAA, 1996.

[6]Kopp, F., "Wake Vortex Characteristics of Military-Type Aircraft Measured at Airport Oberpfaffenhofen Using the DLR Laser Doppler Anemometer," *Aerospace Science and Technology*, , No. 4, 1999, pp. 191–199.

[7]Leishman, G., *Principles of Helicopter Aerodynamics*, New York, NY, 2nd ed., 2006.

[8]Beddoes, T., "A Wake Model for High Resolution Airloads," *U.S. Army/AHS Conference on Rotorcraft Basic Research*, February 1985.

[9]Leishman, J., Bhagwat, M., and Bagai, A., "Free-Vortex Filament Methods for the Analysis of Helicopter Rotor Wakes," *Journal of Aircraft*, Vol. 39, No. 5, 2002, pp. 759–775.

[10]Steijl, R. and Barakos, G., "Sliding Mesh Algorithm for CFD Analysis of Helicopter Rotor-Fuselage Aerodynamics," *International Journal for Numerical Methods in Fluids*, Vol. 58, No. 5, 2008, pp. 527–549.

[11]ANSYS., "ICEM CFD User Manual, Version V14.1," 2011.

[12]Heyson, H. H., "Analysis and Comparison with Theory of Flow Field Measurements Near a Lifting Rotor in the Langley Full-Scale Tunnel," Tech. Rep. NACA TN 3691, NASA, 1956.

[13]Komerath, N., Smith, M., and Tung, C., "A Review of Rotor Wake Physics and Modeling," *Journal of American Helicopter Society*, Vol. 56, No. 2, 2011, pp. 1–19.

[14]Matayoshi, N., Asaka, K., and Okuno, Y., "Flight Test Evaluation of a Helicopter Airborne Lidar," *Journal of Aircraft*, Vol. 44, No. 5, Sept. 2007, pp. 1712–1720.

[15]Padfield, G. and White, M., "Flight Simulation in Academia - HELIFLIGHT in Its First Year of Operation at the University of Liverpool," *The Aeronautical Journal*, Vol. 107, No. 1075, 2003, pp. 529–538.

[16]Padfield, G., Manimala, B., and Turner, G., "A Severity Analysis for Rotorcraft Encounters with Vortex Wakes," *Journal of American Helicopter Society*, Vol. 49, No. 4, 2004, pp. 445–456.

[17]DuVal, R., "A Real-Time Multi-Body Dynamics Architecture for Rotorcraft Simulation, The Challenge of Realistic Rotorcraft Simulation," *RAeS Conference, London*, November 2001.

[18]Advanced Rotorcraft Technology Inc., "FLIGHTLAB Flight Dynamic Models, Version V14," 2013.

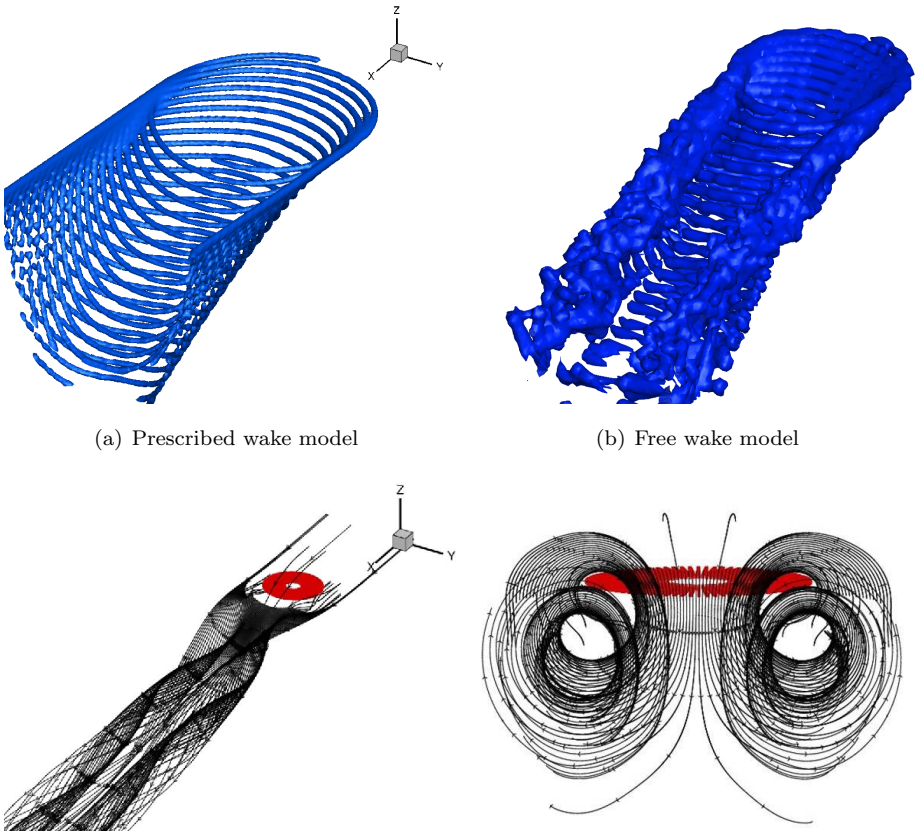

(a) Prescribed wake model

(b) Free wake model

(c) AD model

(d) AD model

Figure 1. Wake vorticity plots (a) and (b), wake stream-lines plots (c) and (d). Four-bladed rotor, C_t=0.013 ;μ=0.1 and α_{TPP}=-4°.

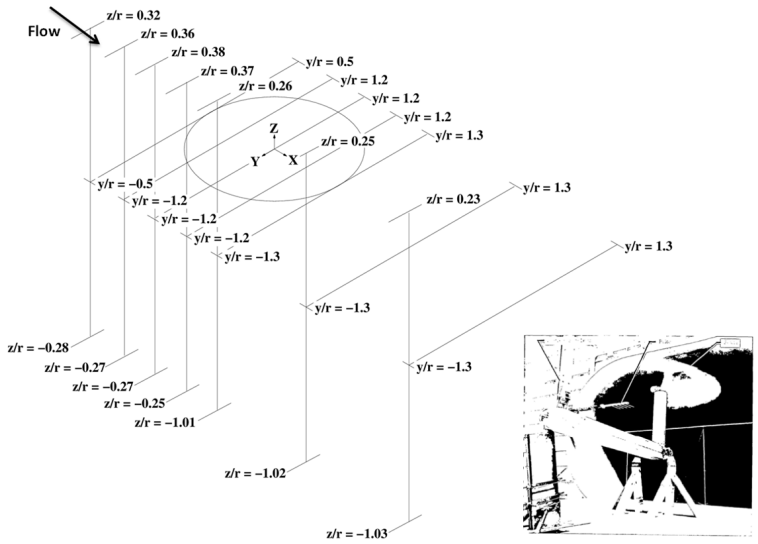

Figure 2. Heyson's wind tunnel rotor wake test set-up and the positions of velocity measurement planes [12].

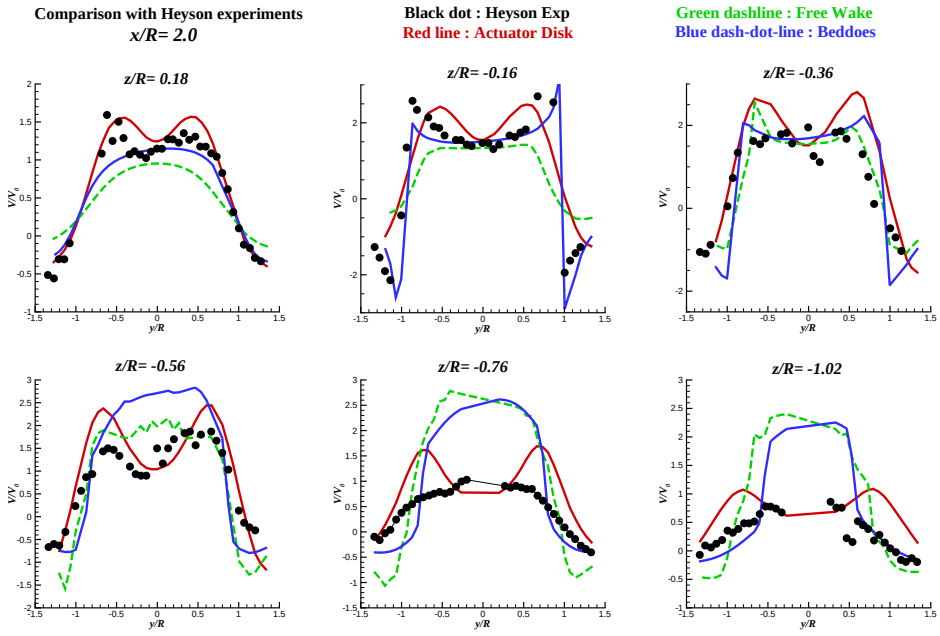

(a) x/R=2.0

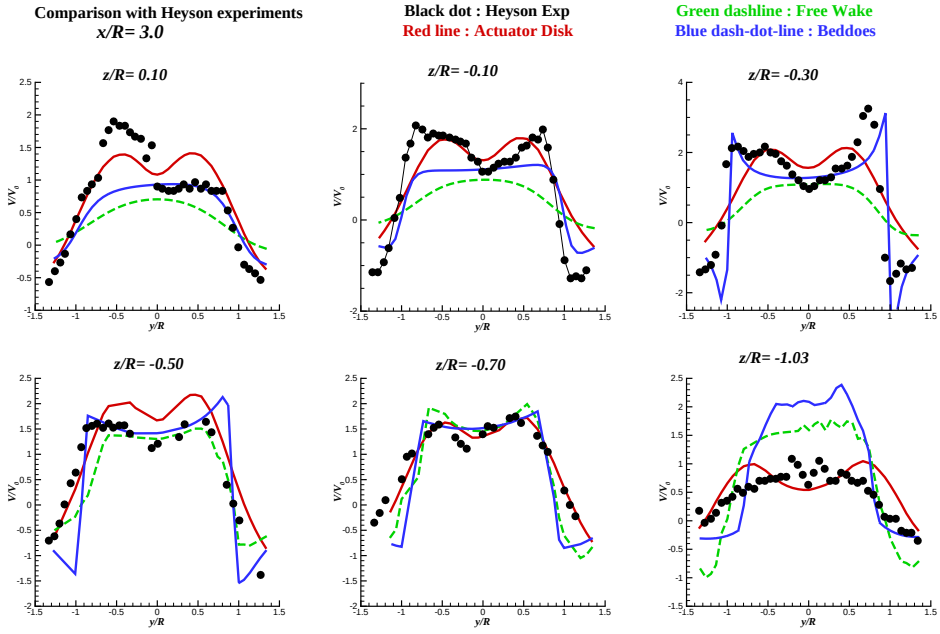

(b) x/R=3.0

Figure 3. Comparison of three wake models against Heyson's experiments[12] at (a) x/R=2 and (b) $x/R = 3$ planes. C_t=0.0064 and μ=0.095.

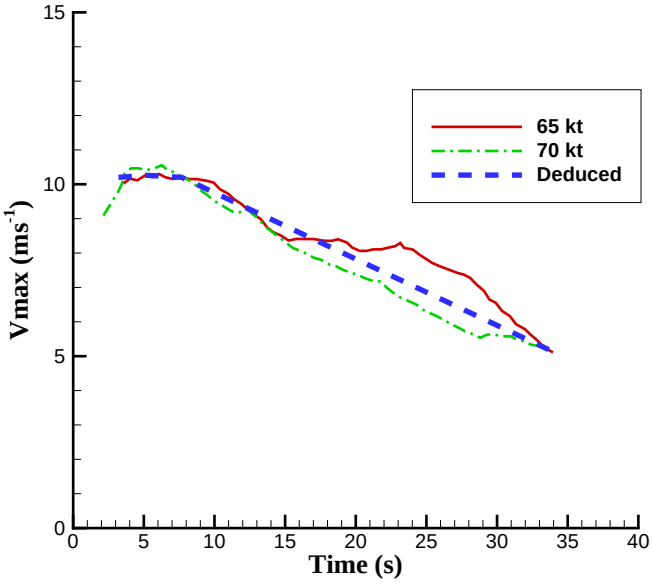

Figure 4. Measured velocity versus vortex age.[6] Puma helicopter at speeds of 65 kt and 70 kt.

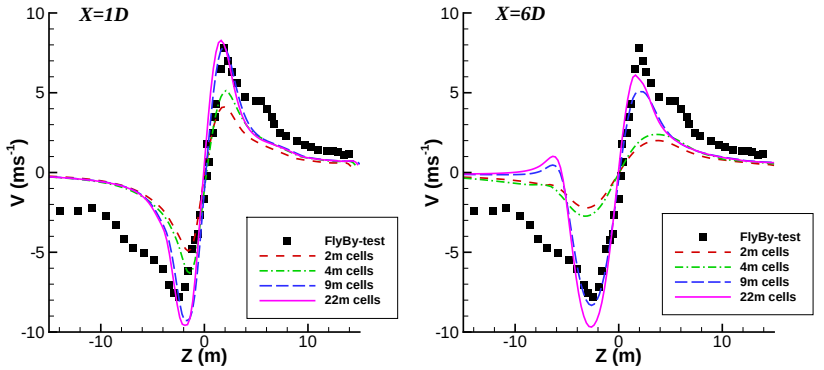

(a) CFD actuator disk model

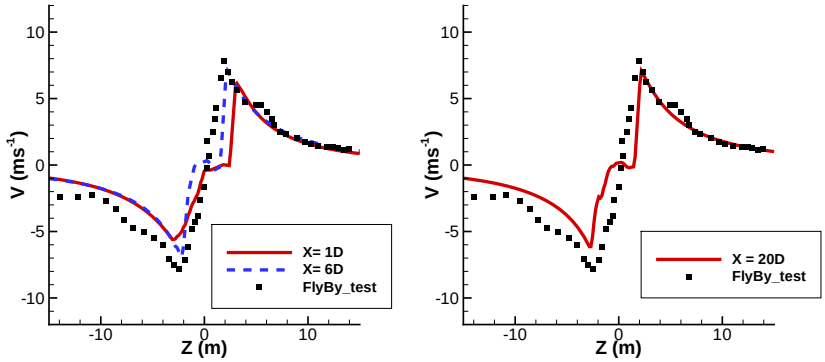

(b) Beddoes wake model with the measured decay relation

Figure 5. Velocity distributions predicted by (a) CFD actuator disk and (b) Beddoes wake model with the measured decay relation. Puma helicopter at speed of 65 kt.

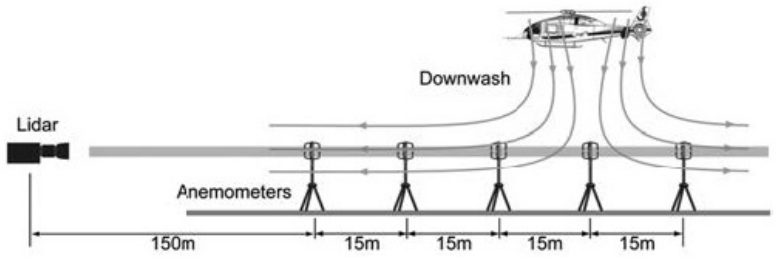

(a) Downwash velocity measurement settings of a hovering MuPAL-ϵ helicopter.[14]

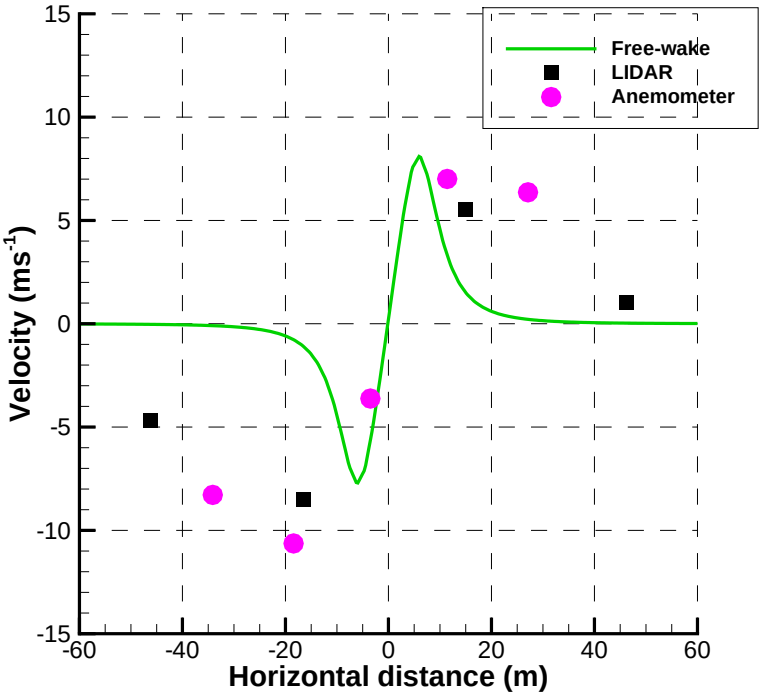

(b) Comparison of wake velocities.

Figure 6. (a) Downwash velocity measurements and (b) comparison of velocities with free wake model. Four-bladed MuPAL-ϵ helicopter with a mass of 4500 kg, hovering at 60-80 ft above ground.

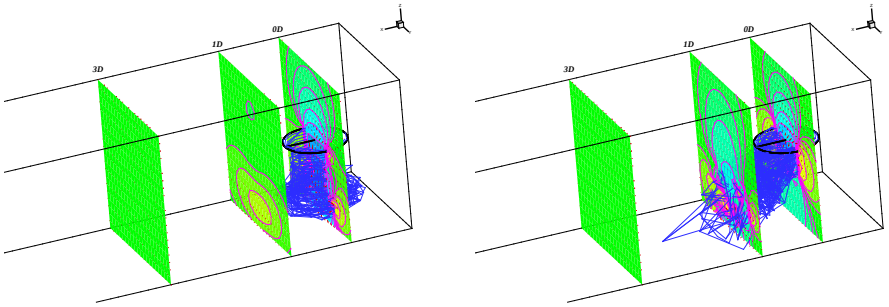

(a) μ=0.0 (b) μ=0.05

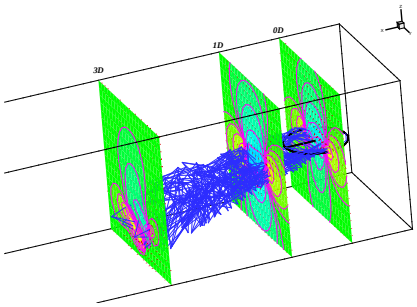

(c) μ=0.1

Figure 7. Contours of downwash velocity and locations of tip vortices generated by the free wake model at (a)μ=0.0 (hover), (b)μ=0.05 and (c)μ=0.1. Dauphin rotor at C_t=0.013, h=50 ft.

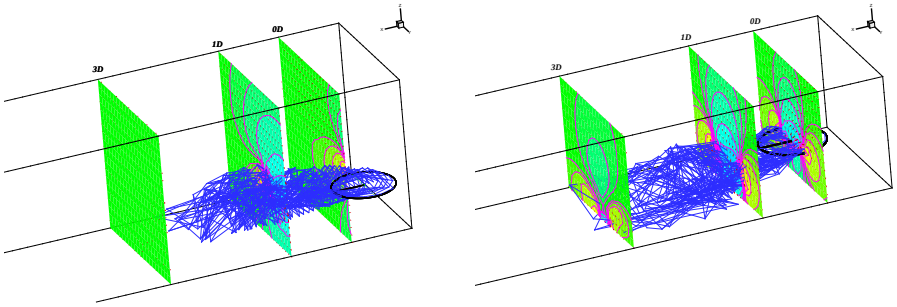

(a) β=45^o, Offset=2D, h=50 ft (b) h=20 ft

Figure 8. Contours of downwash velocity and locations of tip vortices generated by the free wake model. Dauphin rotor C_t=0.013, μ=0.1

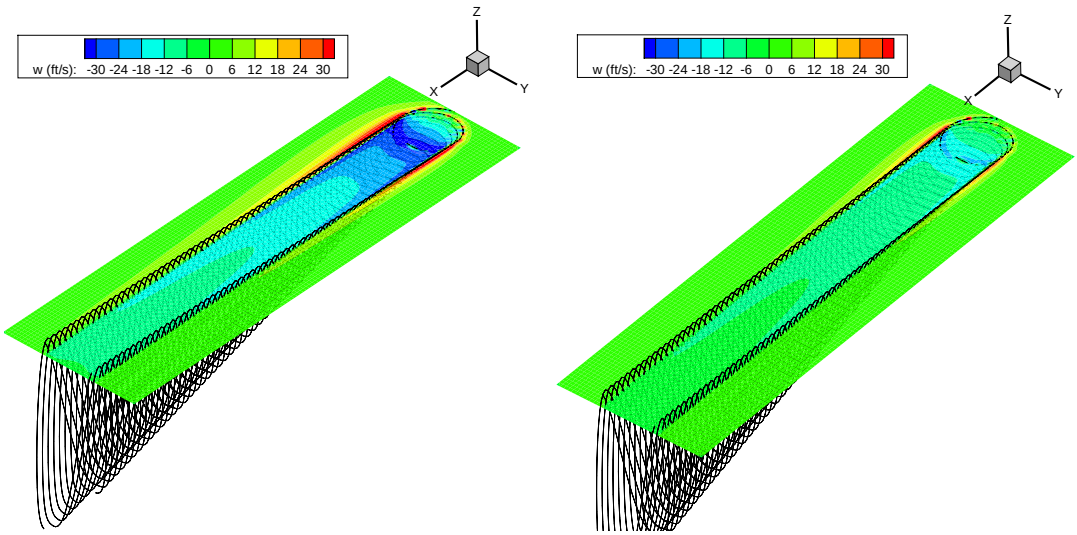

(a) No wake decay (baseline) (b) 50% wake decay

Figure 9. Contours of the induced velocity and wake geometry generated by Beddoes wake model for (a) baseline and (b) 50% wake decay. Dauphin rotor at height of 200 ft, C_t=0.013, μ=0.1.

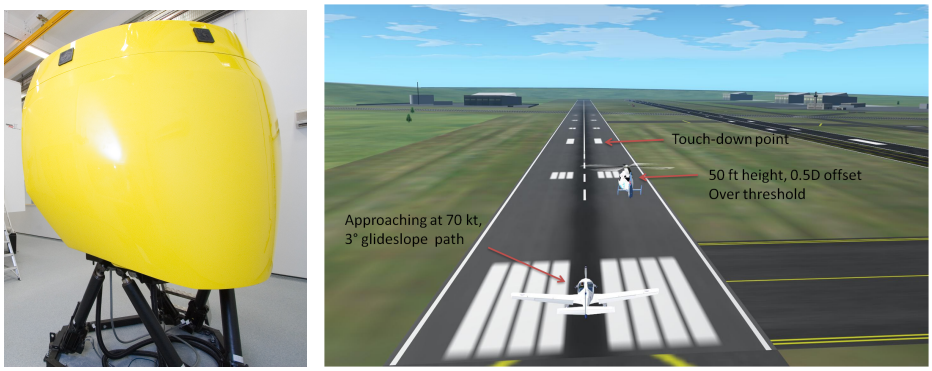

(a) HELIFLIGHT simulator (b) Simulation scene

Figure 10. HELIFLIGHT simulator and the wake encounter simulation scene.

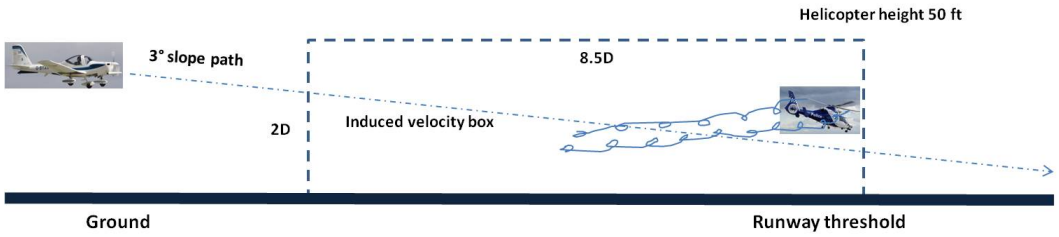

Figure 11. Schematic of the GA aircraft flight path and wake encounter.

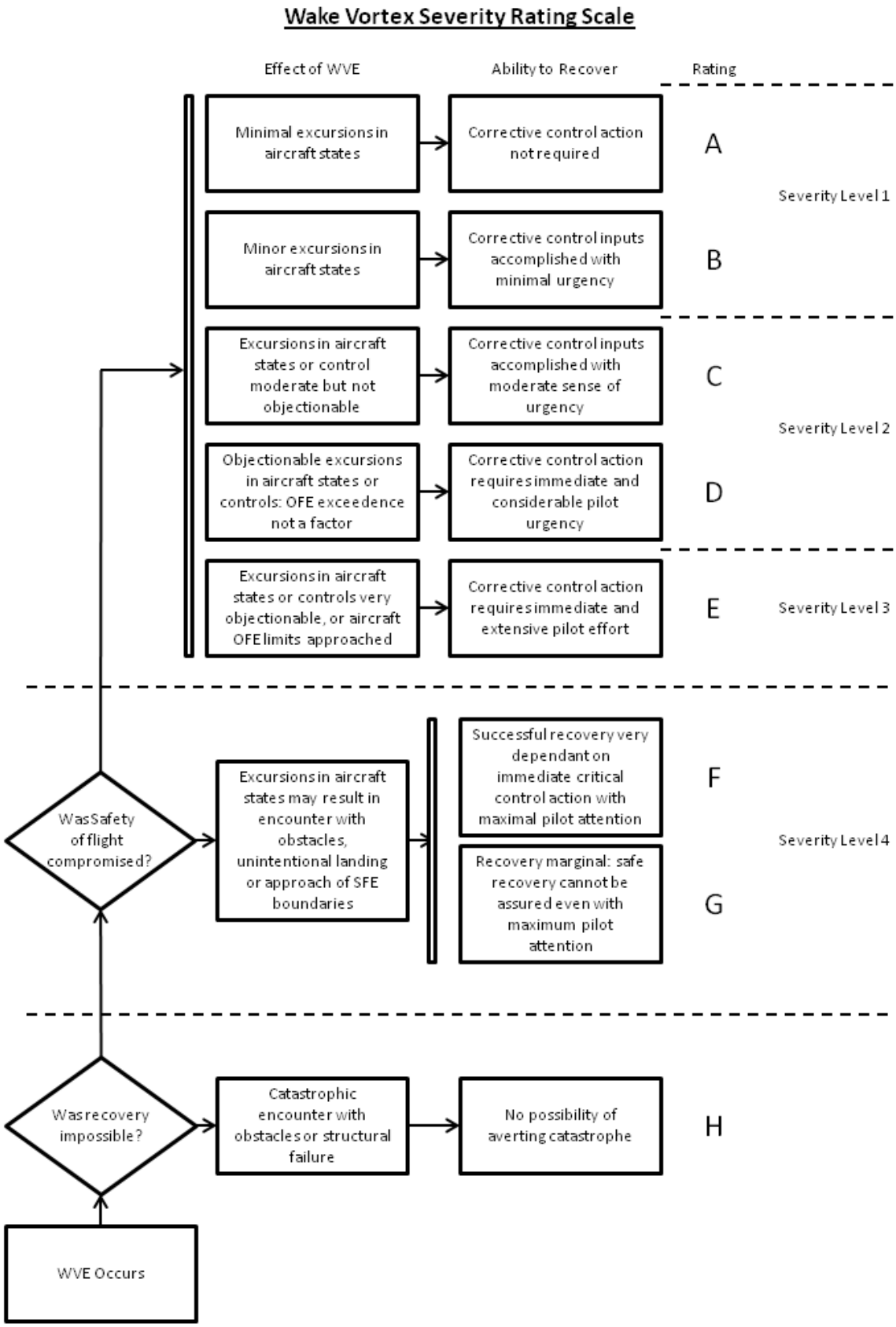

Figure 12. Pilot wake encounter severity rating scale [16].

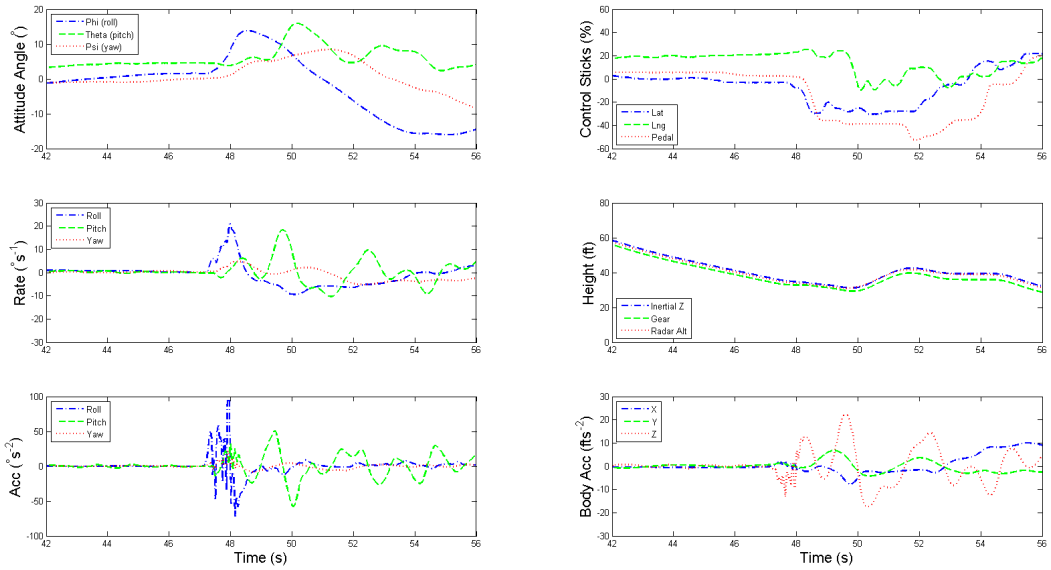

Figure 13. Dynamic responses of GA aircraft and pilot's controls during wake encounter. Helicopter h=50 ft, μ=0.1, β=0°, offset=0.

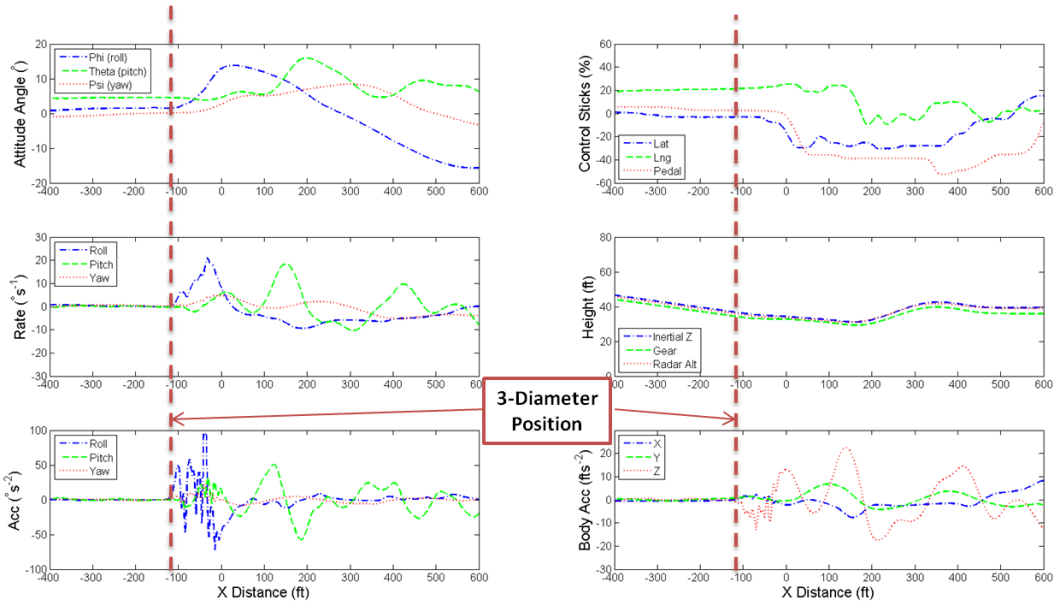

Figure 14. Dynamic responses of GA aircraft and pilot's controls during wake encounter. Helicopter h=50 ft, μ=0.1, β=0°, offset=0.

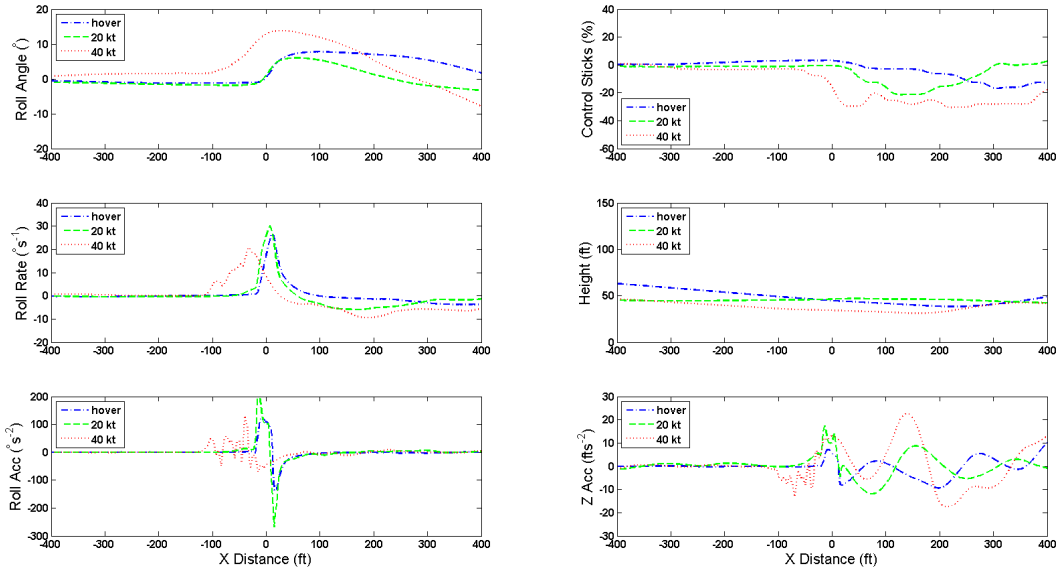

Figure 15. Dynamic responses of GA aircraft and pilot's controls during wake encounter. Helicopter h=50 ft, speed= 0, 20, 40 kt, β=0^o, offset=0.

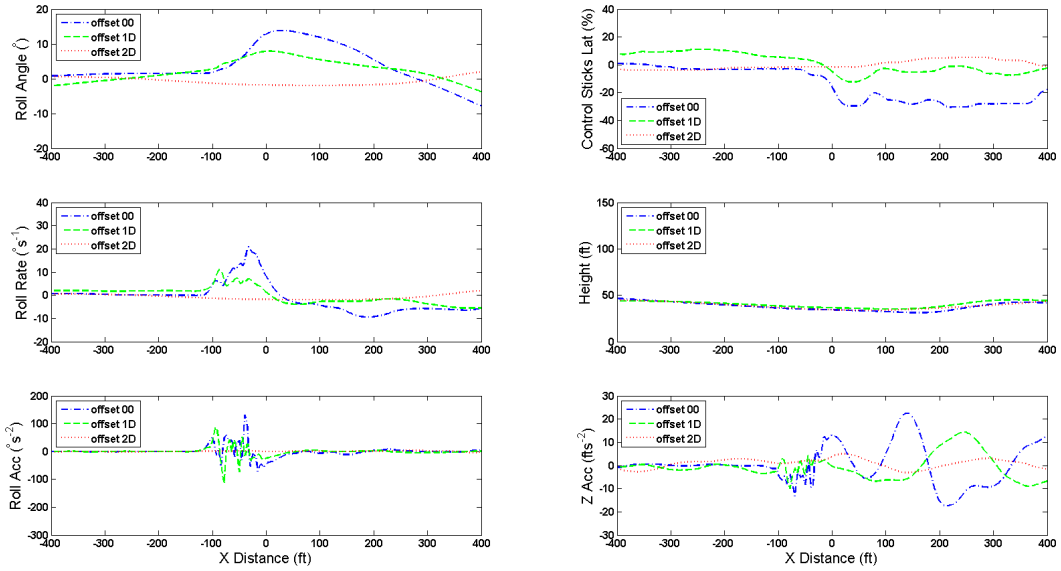

Figure 16. Dynamic responses of GA aircraft and pilot's controls during wake encounter. Helicopter h=50 ft, μ=0.1, β=0^o, offset=0, 1D, 2D.

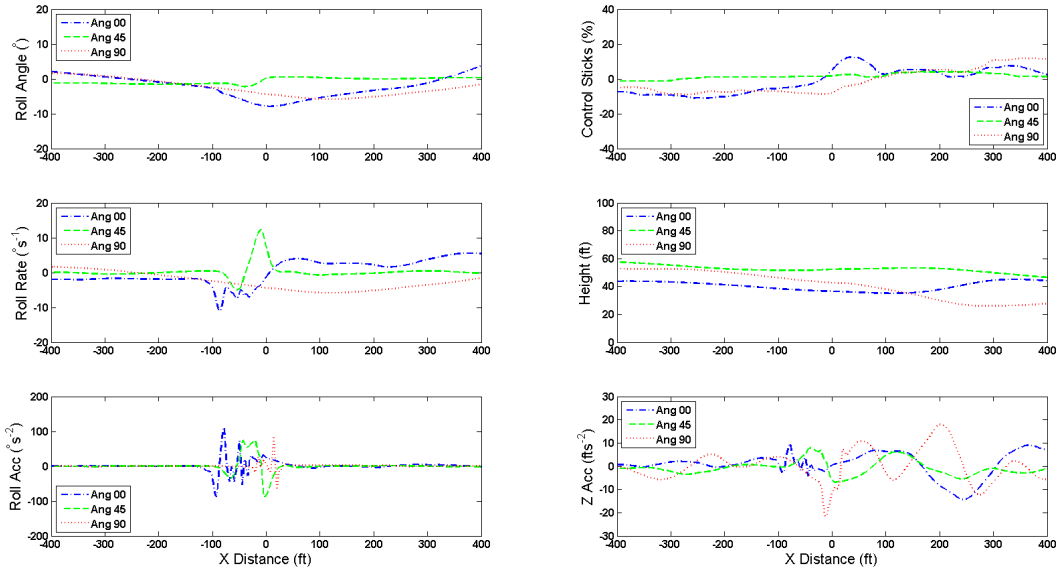

Figure 17. Dynamic responses of GA aircraft and pilot's controls during wake encounter. Helicopter h=50 ft, μ=0.1, β=0^o, 45^o, 90^o. offset=1D.

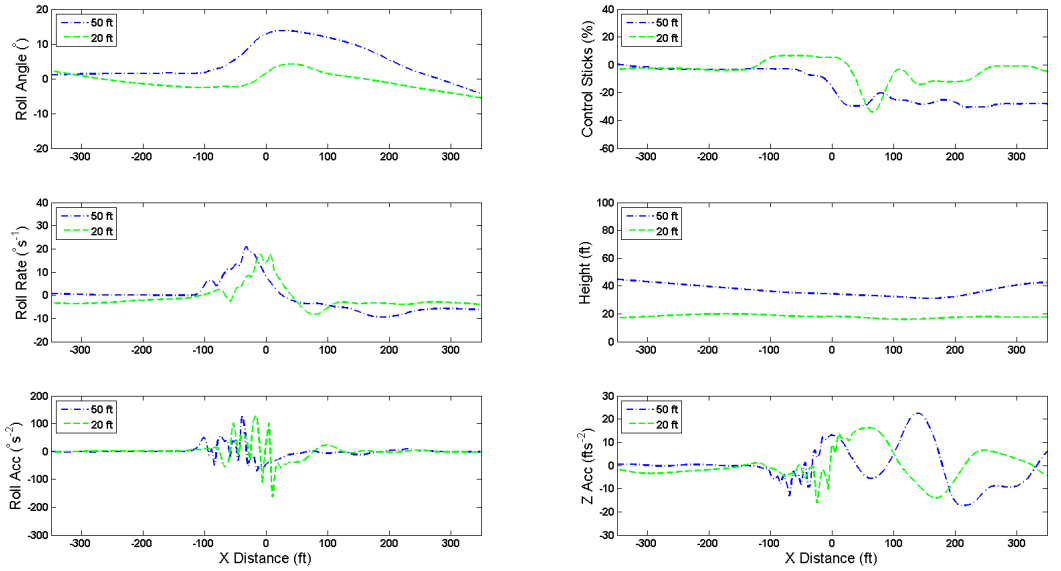

Figure 18. Dynamic responses of GA aircraft and pilot's controls during wake encounter. Helicopter μ=0.1, β=0^o, offset=0, h=50 ft, 20 ft.

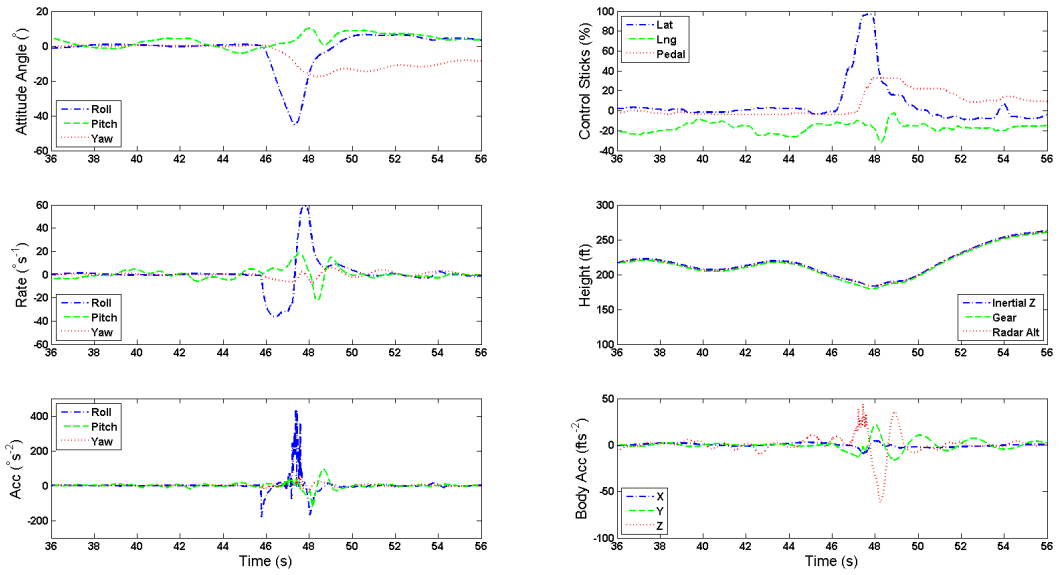

Figure 19. Dynamic responses of GA aircraft and pilot's controls during level flight wake encounter. Helicopter h=200 ft, μ=0.15.

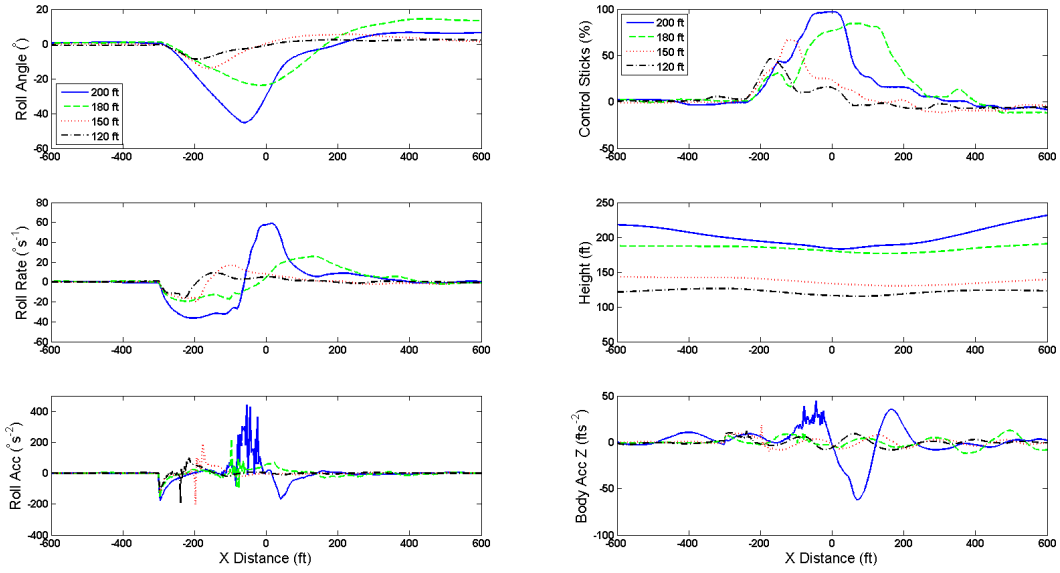

Figure 20. Dynamic responses of GA aircraft and pilot's controls during level flight wake encounter. Helicopter h= 200 ft, μ=0.15, GA aircraft altitude = 200, 180, 150, 120 ft.

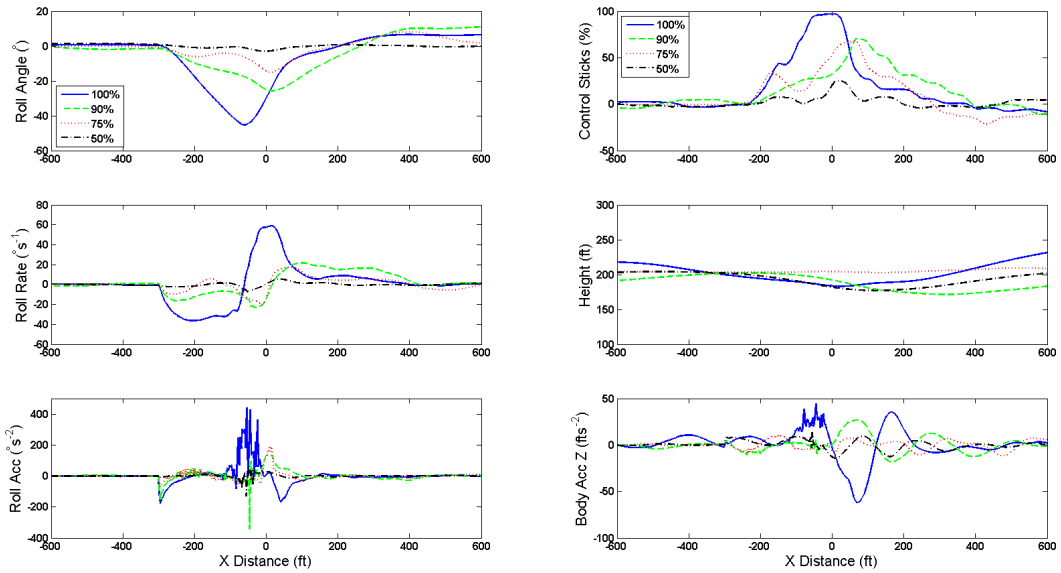

Figure 21. Dynamic responses of GA aircraft and pilot's controls during level flight wake encounter. Helicopter h=200 ft, μ=0.15, wake decay of 100%, 90%, 75% and 50%.